

Comparative analysis of shoreline dynamics in Surabaya and Sidoarjo under climate variability

Eko Hadi Santoso^{1,2*} and Lalu Muhamad Jaelani¹

¹Department of Geomatics Engineering, FTSPK, ITS, Surabaya, East Java, Indonesia

²Maritim Meteorological Station of Tanjung Perak, BMKG, Surabaya, East Java, Indonesia

*Corresponding author: eko.santoso@bmgk.go.id

Abstract. This study investigates the influence of hydroclimatic variability on shoreline dynamics along two contrasting coastal systems in East Java, Indonesia, Surabaya's engineered urban coast and Sidoarjo's natural tidal-flat coast, during 2015–2025. Shorelines were extracted from multi-temporal Landsat imagery using NDWI, shoreline change rates were calculated with DSAS, and rainfall data from BMKG were correlated with mean End Point Rate (EPR) to assess hydroclimatic impacts on coastal morphodynamics. Results reveal contrasting shoreline trajectories driven by coastal typology. Surabaya exhibits semi-cyclic shoreline adjustments controlled by reclamation barriers and restricted sediment pathways, resulting in localized accretion despite declining rainfall. In contrast, Sidoarjo shows rainfall-responsive erosion–accretion cycles, where open tidal channels enable rapid sediment redistribution during high-rainfall periods. Rainfall–EPR correlations are strong at the local scale ($r = 0.76$ in Surabaya; $r = 0.80$ in Sidoarjo) but weak when aggregated ($r \approx 0.10$). This indicates that integrating hydroclimatic indicators with geomorphic context does not increase overall correlation strength, but improves interpretation of typology-specific shoreline responses obscured in aggregated analyses. The NDWI–DSAS–rainfall workflow provides a scalable framework for monitoring shoreline dynamics in tropical monsoonal environments.

Keywords: shoreline dynamics; rainfall variability; NDWI; EPR; Landsat imagery; climate variability, coastal management

1. Introduction

Coastal zones represent dynamic interfaces where natural processes and human interventions continuously reshape geomorphic configurations [1]. Among the various indicators of coastal change, shoreline dynamics are particularly significant, reflecting the cumulative effects of hydrodynamic, climatic, and anthropogenic factors over time [2]. Globally, nearly one-quarter of sandy shorelines are retreating due to sea-level rise, storms, and land-use modification [3]). However, in tropical monsoonal regions such as Indonesia, rainfall variability exerts an additional and often dominant control on sediment transport and coastal morphology [4].

Rainfall influences shoreline evolution primarily through its control on sediment delivery via river discharge and surface runoff, which together determine the magnitude of sediment available for coastal deposition or erosion [5]. Intense precipitation enhances sediment supply to estuarine and coastal zones, promoting accretion, while prolonged dry conditions reduce sediment input and increase susceptibility to tidal erosion. However, this relationship has rarely been quantified explicitly, particularly across contrasting coastal typologies.

In Indonesia, Surabaya and Sidoarjo exemplify two distinct coastal systems shaped by differing geomorphic and anthropogenic conditions. Surabaya's urban coastline is characterized by extensive port development, reclamation, and engineered drainage networks that constrain sediment transport [6]. Conversely, Sidoarjo's tidal-flat coast

remains more natural, dominated by sediment-laden inflows from the Porong River and tidal mixing within aquaculture zones. These contrasting conditions provide an ideal natural laboratory for examining how climatic variability interacts with coastal morphology under different levels of human modification.

Remote sensing has transformed shoreline monitoring by providing synoptic, repeatable, and cost-effective observations across time [7]. Landsat imagery, with its consistent temporal archive since the 1980s, offers a valuable resource for detecting decadal-scale shoreline trends [8]. This study utilizes Landsat 8 Operational Land Imager (OLI) and Landsat 9 OLI-2 surface reflectance products, selected for their radiometric consistency, moderate spatial resolution (30 m), and suitability for long-term shoreline analysis at regional scales. The Normalized Difference Water Index (NDWI), proposed by McFeeters (1996), enhances spectral contrast between land and water, enabling robust shoreline delineation under variable environmental conditions. When integrated with the Digital Shoreline Analysis System (DSAS) developed by the U.S. Geological Survey [9], quantitative metrics such as the End Point Rate (EPR) can be derived to assess erosion–accretion dynamics over time.

Despite technological advances, tropical coastal studies often focus on sea-level rise or anthropogenic stressors, with limited integration of hydroclimatic parameters like rainfall [10]. As a result, the interaction between rainfall-driven hydrological inputs and coastal morphodynamics in monsoonal environments remains poorly understood, especially where river discharge variability and tidal mixing strongly influence sediment pathways. This gap limits predictive modeling capacity and the formulation of climate-informed management strategies.

This study addresses that gap through an integrative, data-driven framework that combines NDWI-based shoreline extraction, DSAS EPR computation, and rainfall correlation analysis to quantify rainfall-induced shoreline dynamics in East Java. Specifically, this study aims to assess decadal shoreline change rates (2015–2025) in Surabaya and Sidoarjo using multi-temporal Landsat data, evaluate the statistical relationship between rainfall variability and shoreline movement, and derive typology-specific insights to support climate-resilient coastal management.

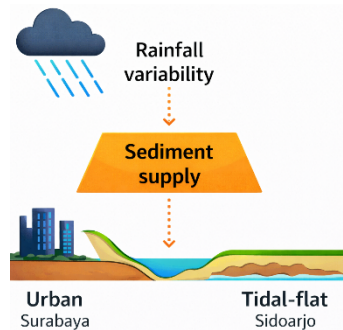


Fig. 1. Conceptual framework linking rainfall variability, sediment supply, and shoreline response in urban (Surabaya) and tidal-flat (Sidoarjo) coastal systems.

The research contributes conceptually and methodologically by embedding rainfall—a climatic proxy—within the geospatial analysis of shoreline change. By contrasting urban and tidal-flat coasts, the study enhances understanding of how hydroclimatic and anthropogenic forces jointly influence tropical coastal evolution. Figure 1 presents the conceptual framework linking rainfall variability, inferred sediment redistribution processes, and shoreline response. Within this framework, rainfall variability is represented by BMKG rainfall records, shoreline response is quantified using NDWI-derived shorelines

and End Point Rate (EPR) metrics from DSAS, while sediment-related processes are interpreted conceptually based on spatial erosion–accretion patterns and coastal typology differences.

Through this framework, the paper bridges geomorphological theory, remote sensing analytics, and applied climate adaptation, offering actionable insights for sustainable coastal governance in data-limited tropical regions.

2. Materials and Methods

2.1 Study Area

The study focuses on two contrasting coastal systems located along the northern coast of East Java, Indonesia: Surabaya (urban coast) and Sidoarjo (tidal-flat coast). Both are situated between 7°19′–7°58′S and 112°45′–112°88′E (Figure 2). Surabaya’s shoreline has been heavily modified by reclamation, harbor dredging, and industrial expansion, resulting in fragmented sediment pathways. In contrast, Sidoarjo’s coast comprises tidal flats and aquaculture ponds that remain geomorphically active, shaped by sediment input from the Porong River and monsoonal tides. The region experiences a tropical monsoon climate with a wide range of annual rainfall (up to ~2,500 mm/year), as reported by BMKG (2024) for Java. BMKG further notes that high precipitation in East Java is linked with large-scale climate drivers, including the Asian–Australian monsoon and ENSO variability [11–12].

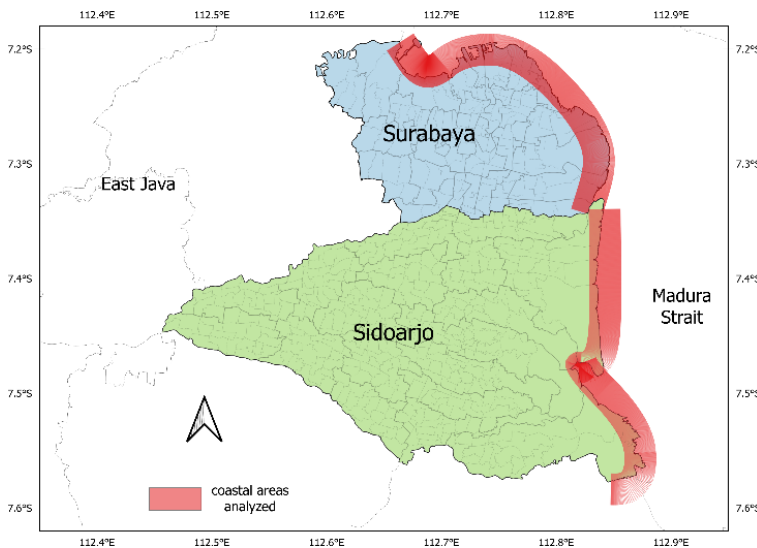


Fig. 2. Study area of Surabaya (urban coast) and Sidoarjo (tidal-flat coast) along the northern coast of East Java, Indonesia.

2.2 Data Acquisition

Table 1. Summary of datasets and their applications.

Data Type	Source	Resolution	Period	Application
Landsat 8 OLI	USGS EarthExplorer	30 m	2015–2021	Shoreline extract
Landsat 9 OLI/TIRS	USGS EarthExplorer	30 m	2022–2025	Shoreline extract
Rainfall data	BMKG (Tanjung Perak, Juanda)	Monthly	2015–2025	Hydroclimatic correlation

Three main datasets were used (Table 1):

- a. Landsat 8 OLI (2015, 2020) and Landsat 9 OLI/TIRS (2025) imagery were obtained from USGS EarthExplorer at 30 m spatial resolution. The analysis utilized visible and near-infrared spectral bands, specifically Band 2 (Blue), Band 3 (Green), Band 4 (Red), and Band 5 (Near-Infrared), which are commonly employed for shoreline extraction and land–water discrimination. Images were selected under cloud cover less than 10%, based on USGS metadata, and atmospherically corrected prior to analysis.
- b. Rainfall data from BMKG’s Tanjung Perak (Surabaya) and Juanda (Sidoarjo) stations, representing urban and tidal-flat rainfall regimes from 2015–2025. Monthly rainfall was aggregated into annual totals.
- c. Supporting datasets, including shoreline baselines and administrative boundary maps, were obtained from open-access national geospatial sources, specifically the Geospatial Information Agency of Indonesia (Badan Informasi Geospasial, BIG). These datasets were used for georeferencing, spatial alignment, and interpretation of shoreline changes.

2.3 Shoreline Extraction using NDWI

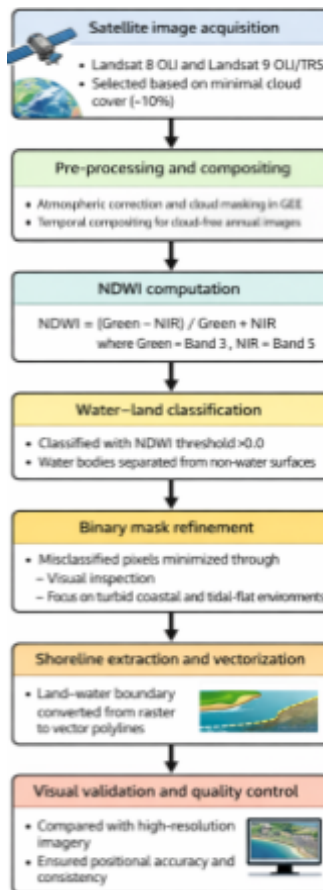


Fig. 3. Detailed workflow of NDWI-based shoreline extraction and validation using Google Earth Engine, including image pre-processing, NDWI thresholding, shoreline vectorization, and visual quality control.

Shoreline positions were delineated using the Normalized Difference Water Index (NDWI) [13]:

$$NDWI = \frac{Green - NIR}{Green + NIR} \tag{1}$$

where Green and NIR represent surface reflectance values from Landsat Band 3 and Band 5. Processing was implemented on Google Earth Engine (GEE), ensuring radiometric consistency and cloud-free composites. Pixels were classified using an NDWI threshold of > 0.0 , a commonly adopted criterion for distinguishing water from non-water surfaces in Landsat-based coastal studies, as positive NDWI values indicate the dominance of water reflectance characteristics. The threshold was empirically verified through visual calibration against high-resolution reference imagery to ensure robust land–water separation under varying tidal and atmospheric conditions. The extracted shorelines were visually validated against high-resolution imagery to ensure positional reliability.

2.4 Shoreline Change Rate Analysis

The Digital Shoreline Analysis System (DSAS) v6.0 was used to compute shoreline change rates via the End Point Rate (EPR) method [9]:

$$EPR = \frac{D_2 - D_1}{T} \tag{2}$$

where D_1 and D_2 are shoreline positions (m) at times t_1 and t_2 , and T is the elapsed time (years). A baseline was generated parallel to the coast, and transects were spaced every 30 m — totaling 1,015 in Surabaya and 984 in Sidoarjo. EPR values (m/year) were categorized into erosion (negative), accretion (positive), or stable (± 0.5 m/year).

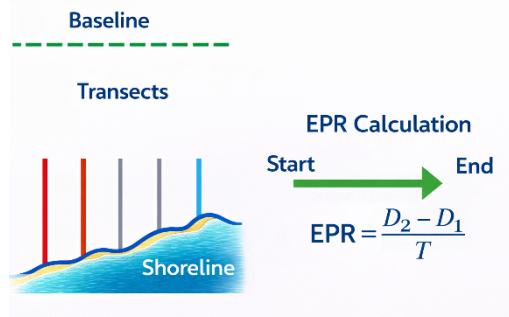


Fig. 4. DSAS analytical framework showing baseline, transects, and EPR calculation workflow.

2.5 Rainfall–Shoreline Correlation Analysis

To quantify the climatic influence, Pearson’s correlation coefficient (r) was applied to assess the relationship between annual rainfall totals and mean EPR values (2015–2025):

$$r = \frac{\sum(x_i - \bar{x})(y_i - \bar{y})}{\sqrt{\sum(x_i - \bar{x})^2 \sum(y_i - \bar{y})^2}} \tag{3}$$

where x represents annual rainfall and y represents EPR. Statistical analysis was performed using Excel.

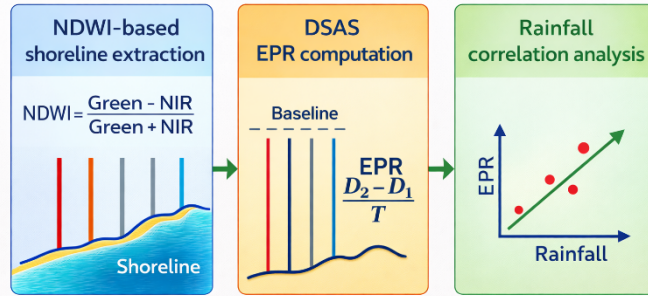


Fig. 5. Research workflow integrating NDWI-based shoreline extraction, DSAS EPR computation, and rainfall correlation analysis.

3. Results and Discussion

3.1 Shoreline Dynamics Overview (2015–2025)

Multi-temporal analysis revealed distinct morphodynamic responses between the two coasts.

- Surabaya: EPR values ranged from -67.5 to $+120$ m/year (mean = $+4.5$ m/year). Approximately 28% of transects indicated erosion, 41% accretion, and 31% stability. Erosional hotspots were concentrated near Benowo (Tambak Oso Wilangun), Krembangan (Perak Barat), and Pabean Cantian (Perak Utara), as highlighted in Figure 6, while localized accretion prevailed along Bulak and Sukolilo Baru. The spatial distribution of these erosion–accretion patterns reflects the combined influence of coastal infrastructure development, modified drainage networks, and sediment trapping by nearshore structures.

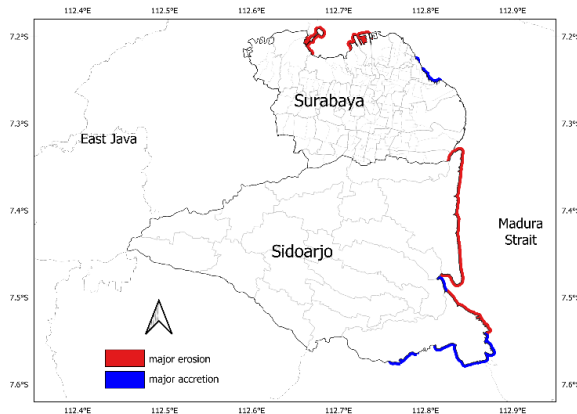


Fig. 6. Spatial distribution of shoreline change rates (EPR) along the Surabaya and Sidoarjo coast from 2015 to 2025.

- Sidoarjo: EPR values ranged from -179 to $+189$ m/year (mean = -1.6 m/year). Nearly 47% of transects experienced erosion, especially in Sedati (Kalanganyar and Segorotambak) and Jabon (southern Kupang), while 32% accretion occurred in northern Kupang and Kedungpandan, reflecting sediment accumulation within tidal channels but insufficient to offset net coastal retreat.

Surabaya’s engineered shoreline promotes localized progradation due to sediment trapping behind coastal structures. In contrast, Sidoarjo’s open tidal plain remains highly susceptible to erosion because hydrodynamic energy and reduced sediment supply act more freely across the system. These contrasting morphologies reflect how human modification in Surabaya constrains sediment mobility, while tidal processes in Sidoarjo amplify natural morphodynamic variability [2], [5].

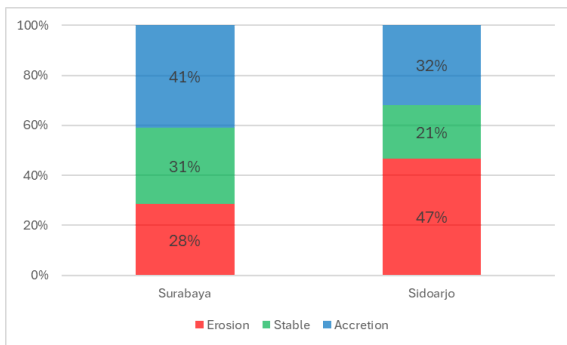


Fig. 7. Comparative distribution of erosion, accretion, and stable shoreline segments in Surabaya and Sidoarjo (2015–2025).

3.2. Rainfall Variability and Shoreline Response

Annual rainfall ranges from 1,371 mm/year (2023–2025) in Surabaya to 2,370 mm/year (2015–2017 and 2019–2020) in Sidoarjo. Correlation analysis revealed coast-specific relationships between rainfall variability and shoreline change, as illustrated in Figure 8. For Surabaya, the scatter distribution shows a clear upward trend, where higher annual rainfall generally corresponds to positive EPR values, indicating net accretion ($r = 0.76$). Similarly, Sidoarjo exhibits a stronger positive association ($r = 0.80$), characterized by a steeper trend and wider dispersion of EPR values under high-rainfall conditions, reflecting the sensitivity of tidal-flat environments to rainfall-driven sediment redistribution.

In contrast, when data from both regions are combined, the scatter points in Figure 8 become widely dispersed around a near-horizontal regression line ($r = 0.10$), indicating the absence of a consistent rainfall–shoreline response across the study area. This divergence highlights the role of local coastal controls, such as urbanized shore protection in Surabaya and tidal-channel dynamics in Sidoarjo, which modulate how rainfall signals are translated into shoreline change.

Periods of high rainfall corresponded with net accretion (2015–2017, 2019–2021), while dry phases (2017–2019, 2023–2025) coincided with erosion. This finding confirms that rainfall variability acts as a hydroclimatic driver modulating sediment redistribution, though its effect is filtered by coastal typology [4].

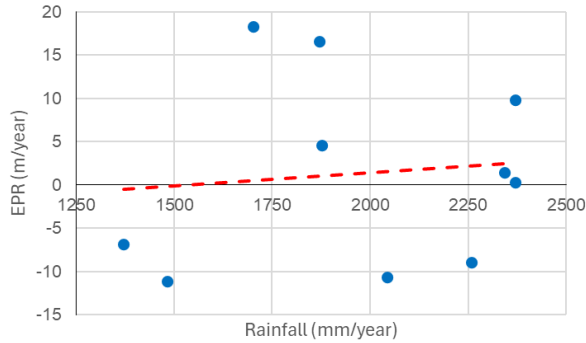


Fig. 8. Scatter plot illustrating the relationship between annual rainfall and shoreline change rates (EPR) for the Surabaya and Sidoarjo coasts during 2015–2025.

In Surabaya, rainfall-driven sediment flux was weakened by engineered drainage and reclamation barriers, leading to localized accretion near confined basins but resulting in overall morphological rigidity. In Sidoarjo, the open tidal system responded more directly—high rainfall enhanced fluvial sediment input, promoting widespread accretion, whereas low rainfall reduced sediment supply, increasing tidal erosion [14]. This spatially divergent behavior explains why rainfall–EPR correlations remain strong locally but lose coherence when both coasts are analyzed together.

3.3. Spatiotemporal Morphodynamic Patterns

Temporal segmentation (2015–2017, 2017–2019, 2019–2021, 2021–2023, 2023–2025) revealed alternating erosion–accretion phases (Figure 9).

- Surabaya exhibited a semi-cyclic behavior, defined here as a recurring but non-periodic alternation between accretion and erosion phases over successive time segments rather than a regular oscillatory cycle. Accretion dominated during 2015–2017 and 2019–2023, whereas erosion prevailed in 2017–2019 and 2023–2025. As shown in Figure 9, these phase transitions coincide with shifts in rainfall regimes and are further modulated by major port reclamation activities along the Surabaya waterfront between 2016 and 2021, which altered sediment pathways and promoted localized sediment trapping behind coastal structures. Consequently, net accretion dominates despite persistent erosion in western sectors.
- Sidoarjo demonstrated a more synchronous response, meaning that shoreline changes occurred consistently and coherently with rainfall variability across the analyzed periods. As illustrated in Figure 9, strong accretion systematically corresponds to high-rainfall phases (2015–2017 and 2019–2023), while pronounced erosion aligns with drier intervals. This close temporal alignment reflects the dominance of tidal-channel-controlled sediment transport and the limited buffering capacity of engineered coastal structures in the Sidoarjo tidal-flat environment.

These results underscore that Surabaya’s morphodynamic pattern is primarily engineering-driven, while Sidoarjo’s evolution remains rainfall-driven, producing opposite shoreline tendencies—net accretion versus net erosion. These cycles demonstrate that rainfall–sediment coupling is more effective in natural tidal systems than in engineered coasts [5-6].

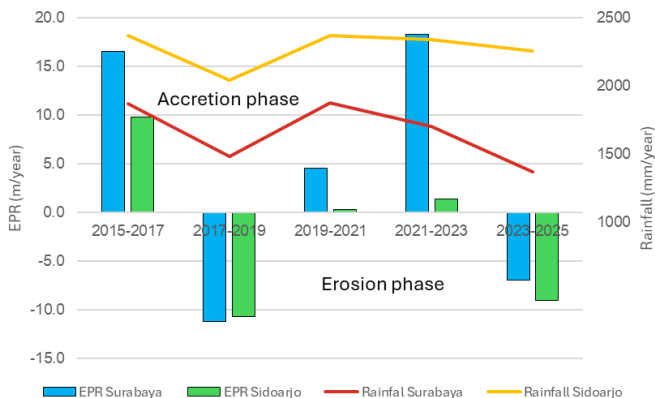


Fig. 9. Temporal evolution of mean EPR and rainfall anomalies showing alternating erosion–accretion phases.

As illustrated in Figure 9, the temporal evolution of mean EPR exhibits a clear alternation between accretion and erosion phases that broadly co-varies with rainfall variability. During 2015–2017, both Surabaya and Sidoarjo experienced positive mean EPR values, coinciding with elevated rainfall, indicating a net accretion phase. This pattern shifted in 2017–2019, when reduced rainfall corresponds to negative mean EPR values at both sites, marking a transition to erosion-dominated conditions.

The accretion phase re-emerged during 2019–2021 and intensified in 2021–2023, particularly in Surabaya, where peak positive EPR values align with above-average rainfall. In contrast, the subsequent period (2023–2025) shows a decline in rainfall accompanied by negative mean EPR values, signaling a renewed erosion phase. The consistent temporal alignment between rainfall peaks and positive EPR, as well as rainfall minima and negative EPR, supports the interpretation of alternating erosion–accretion cycles driven by rainfall-modulated sediment redistribution, with local coastal settings influencing the magnitude of the response.

3.4. Comparative Morphodynamic Interpretation

Table 2. Comparative morphodynamic indicators of Surabaya and Sidoarjo (2015–2025).

Parameter	Surabaya (Urban)	Sidoarjo (Tidal-flat)
Dominant driver	Anthropogenic (reclamation, drainage control)	Hydroclimatic (rainfall, tide, etc)
Mean EPR (m/year)	+4.5	-1.6
Rainfall-EPR Correlation (r)	0.76	0.80
Sediment connectivity	Low (confined by infrastructure)	High (open tidal channels)
Morphodynamic behavior	Localized, delayed response	Immediate, widespread response

The comparative assessment emphasizes that geomorphic openness and human modification jointly determine how rainfall signals manifest in shoreline morphology. As summarized in Table 2, Surabaya shows a net accretion trend, whereas Sidoarjo exhibits net erosion. In the urbanized coast of Surabaya, structural confinement reduces sediment mobility, creating localized accretional zones and overall morphological persistence. In

contrast, Sidoarjo's open tidal system permits more immediate responses to hydroclimatic forcing, translating rainfall decline into accelerated erosion.

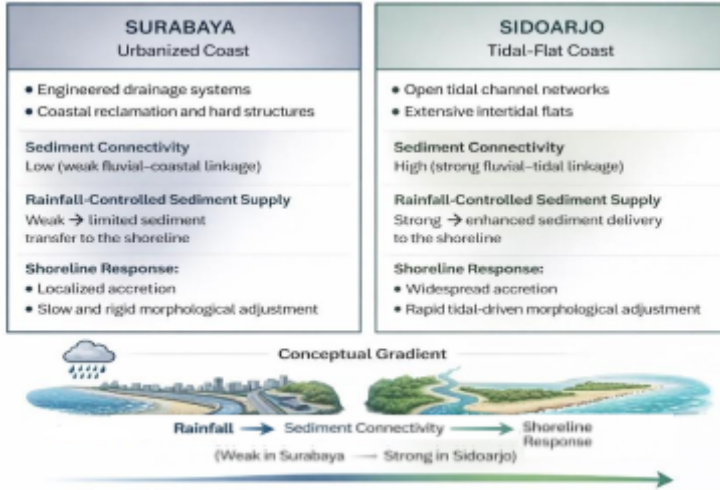


Fig. 10. Conceptual comparison of sediment pathways and rainfall influence in Surabaya vs. Sidoarjo.

While the urban coast gains structural stability at the expense of ecological flexibility, the tidal-flat coast retains dynamic resilience but faces persistent spatial volatility. These opposing behaviors confirm that anthropogenic confinement promotes accretion but suppresses adaptive sediment redistribution, whereas geomorphic openness amplifies erosional risk under reduced rainfall conditions. These contrasts are further clarified through a simplified conceptual comparison illustrating how sediment pathways and rainfall sensitivity differ between the two systems (Figure 10), reinforcing the need for differentiated coastal management strategies.

Specifically, structurally reinforced and maintenance-oriented interventions—such as breakwater optimization, controlled reclamation, and periodic sediment management—are more appropriate for Surabaya, where shoreline behavior is dominated by anthropogenic confinement. In contrast, nature-based and adaptive approaches, including mangrove rehabilitation, tidal-flat conservation, and the preservation of sediment exchange pathways, are better suited for Sidoarjo, where shoreline dynamics respond more directly to rainfall-driven sediment fluctuations. This distinction consistently appears across all temporal segments and underpins the contrasting shoreline behaviors observed in both regions [1], [3].

3.5. Integrated Conceptual Model

Figure 11 synthesizes the observed relationships among rainfall variability, sediment flux, and shoreline response. In Surabaya, the influence of rainfall is strongly mediated by engineered infrastructure and reduced drainage connectivity, producing compartmentalized sediment dynamics and spatially confined accretion. In Sidoarjo, rainfall directly governs sediment transport through tidal channels, intensifying erosion when precipitation declines. This model supports the broader climate-morphodynamic framework, highlighting that hydroclimatic variability is a major but spatially filtered determinant of coastal evolution in tropical regions. Accordingly, the degree of human alteration dictates whether rainfall acts as a stabilizing (urban) or destabilizing (tidal-flat) agent within the shoreline system [4]. However, this apparent stabilization along Surabaya's urban coast may introduce long-term vulnerabilities, as rigid coastal structures can limit landward sediment accommodation and

increase the risk of coastal squeeze under future sea-level rise, potentially reducing the system's adaptive capacity.

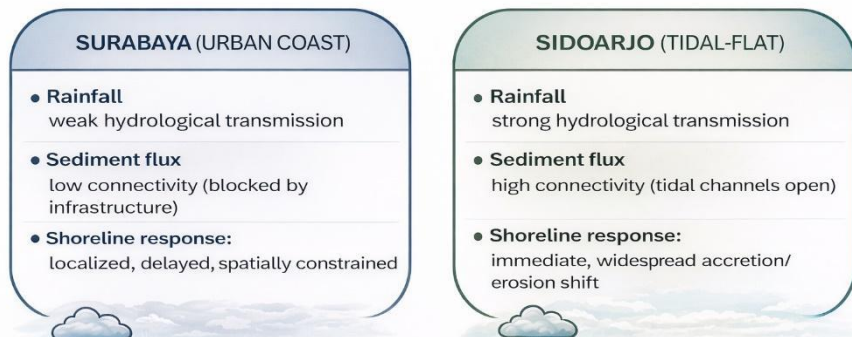


Fig. 11. Integrated conceptual model of rainfall–sediment–shoreline interactions in urban and tidal-flat coastal systems.

4. Conclusions

This study examined shoreline dynamics in two contrasting coastal systems—Surabaya’s urban coastline and Sidoarjo’s tidal-flat coastline—over the period 2015–2025 using multi-temporal Landsat imagery, NDWI-based shoreline extraction, DSAS-derived change rates, and rainfall correlation analysis. The results reveal fundamentally different morphodynamic behaviors governed by geomorphic setting and the degree of human modification.

Surabaya exhibits a predominantly accretional shoreline response (mean EPR = +4.5 m/year), reflecting the influence of reclamation structures, engineered drainage networks, and coastal protection measures. These interventions produce what is referred to here as semi-stable geomorphic conditions, characterized by persistent net accretion combined with reduced short-term shoreline mobility and a dampened response to rainfall variability across successive temporal segments. In contrast, Sidoarjo displays a predominantly erosional regime (mean EPR = -1.6 m/year), where open tidal-flat morphology and active channel networks maintain strong sediment connectivity, allowing rainfall variability to translate directly into alternating erosion–accretion phases.

Correlation analysis further confirms rainfall as a significant climatic driver at the individual-coast scale, with strong positive relationships observed in Surabaya ($r = 0.76$) and Sidoarjo ($r = 0.80$). However, when both coastlines are analyzed together, the relationship weakens substantially ($r \approx 0.10$), demonstrating that aggregation across contrasting geomorphic typologies can obscure hydroclimatic signals. This finding highlights the importance of spatial context when interpreting climate–shoreline interactions in heterogeneous coastal systems.

Overall, the integrated NDWI–DSAS–rainfall framework proved effective for decadal-scale shoreline assessment, enabling robust detection of morphodynamic cycles and sediment–rainfall interactions under data-limited conditions. The study underscores that hydroclimatic variability alone cannot fully explain shoreline evolution in tropical coastal environments; instead, shoreline responses emerge from the combined influence of rainfall forcing, geomorphic openness, sediment connectivity, and human alteration. These insights reinforce the need for coastal management strategies that are explicitly tailored to local morphodynamic settings rather than uniformly applied across regions.

The findings highlight three key points:

- Coastal typology governs sensitivity to rainfall: engineered coasts exhibit morphological stability, whereas tidal-flat coasts demonstrate amplified responses to rainfall fluctuations.
- Rainfall–shoreline coupling is scale-dependent: correlations are strong at local scales but diminish when contrasting coasts are aggregated.
- Sediment connectivity mediates climate forcing: structural confinement reduces system responsiveness, while geomorphic openness increases susceptibility to erosion during low-rainfall years.

5. Implications for Sustainable Coastal Management

The implications of this study span policy, management, and methodological dimensions, reflecting the distinct morphodynamic behavior of Surabaya and Sidoarjo. In highly urbanized coastal settings such as Surabaya, sediment management actions shown in Figure 12 do not imply large-scale natural sediment bypassing. Instead, feasibility is limited to localized and managed sediment redistribution, implemented through periodic dredging at river mouths and port areas followed by controlled placement of sediments to downdrift coastal segments. This approach integrates with existing port maintenance activities and avoids major land-use conflicts while partially restoring sediment continuity.

a. Policy Implications

Urban coasts such as Surabaya require integrated planning that aligns coastal development with sediment system functioning. Reclamation zoning, adaptive drainage design, and sediment bypassing mechanisms are essential to prevent sediment imbalance caused by structural confinement. In highly dense urban settings, sediment bypassing is feasible primarily as a localized and managed intervention, implemented through periodic dredging at river mouths, port entrances, or engineered drainage outlets, followed by controlled sediment placement to downdrift coastal segments. Given that urban sediment connectivity is weak and rainfall–shoreline coupling is limited, policies should prioritize maintaining residual sediment pathways rather than relying on hydroclimatic inputs alone. Incorporating rainfall variability into coastal risk assessments enhances long-term planning under climate uncertainty [6].

b. Ecosystem-Based Management

In natural tidal systems like Sidoarjo, ecosystem-based adaptation (EbA) and nature-based solutions (NbS) can strengthen resilience to rainfall-driven erosion. Strategies may include mangrove rehabilitation, tidal channel conservation, and controlled sediment redistribution. Because sediment connectivity is strong and rainfall–EPR correlation is high, management must preserve hydrological openness to allow sediment transport to continue buffering erosional phases during low-rainfall years. This approach supports dynamic stability without restricting natural morphodynamic processes [14].

c. Methodological Advancement

The integration of NDWI-derived shorelines, DSAS rate metrics, and rainfall analysis demonstrates a scalable and cost-efficient monitoring framework for tropical coasts. The weakened combined correlation ($r \approx 0.10$) indicates that regional shoreline forecasting should avoid aggregating geomorphically different coastlines into unified models; instead, typology-specific modelling improves interpretability and predictive performance. Future work should include wave climate, tidal energy, land subsidence, and anthropogenic sediment interventions, with machine learning approaches (e.g., Random Forest, hybrid neural models) to enhance predictive skill [10].

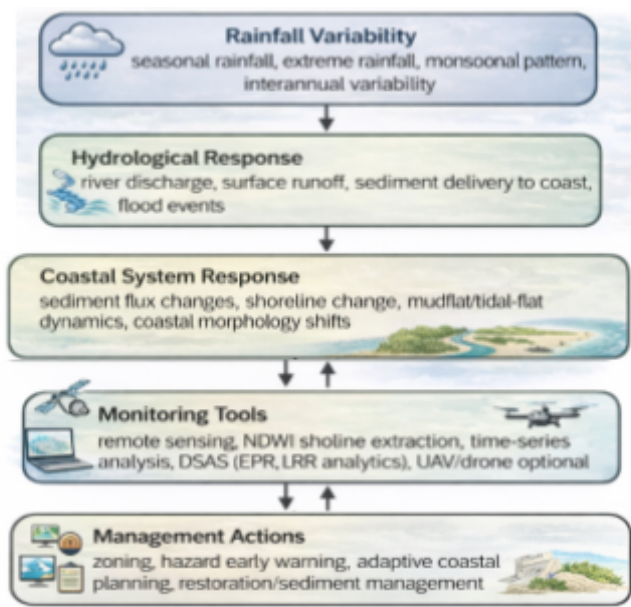


Fig. 12. Framework for integrating rainfall variability into coastal management and monitoring.

This framework highlights that rainfall-driven shoreline responses must be interpreted according to coastal typology, as urban engineered coasts and natural tidal flats react differently to the same hydroclimatic forcing. By linking rainfall anomalies, sediment connectivity, and morphodynamic behavior, it directs managers toward typology-specific adaptation pathways.

The weak combined correlation ($r \approx 0.10$) further indicates that geomorphically distinct coasts should not be merged in regional forecasting; rainfall must be incorporated separately for each coastal type to ensure diagnostic reliability. This integrative approach supports evidence-based decision-making consistent with the Sendai Framework and SDG 13, strengthening climate-resilient coastal governance for Indonesia’s northern shoreline.

6. Limitations and Future Research Directions

The NDWI–DSAS–rainfall framework provides a robust basis for comparing shoreline dynamics across contrasting coastal typologies; however, several methodological and interpretative limitations should be acknowledged. The 30 m spatial resolution of Landsat imagery constrains the detection of fine-scale shoreline changes, particularly within wide intertidal zones. Positional uncertainty associated with shoreline extraction may range from approximately 10 to 30 m, depending on tidal stage, shoreline slope, and image acquisition conditions. This uncertainty directly affects the calculated End Point Rate (EPR), potentially dampening short-term erosion–accretion signals while remaining less influential on decadal-scale trends. Consequently, while absolute EPR magnitudes should be interpreted cautiously, the dominant accretional and erosional tendencies identified for Surabaya and Sidoarjo, respectively, are considered robust at the temporal scale examined.

Residual tidal-phase inconsistencies among multi-temporal images may further influence shoreline positioning, with a greater impact in Sidoarjo’s gently sloping tidal flats where small vertical tidal differences translate into larger horizontal shoreline shifts. In contrast, Surabaya’s engineered coastline exhibits sharper geomorphic boundaries, making shoreline position more sensitive to spatial resolution than to tidal variability.

Although rainfall was treated as the primary hydroclimatic driver, the weak correlation observed when both coastlines were aggregated ($r \approx 0.10$) reflects not merely a limitation of the correlation approach, but a physical dominance of contrasting coastal controls. Aggregation masks rainfall signals because shoreline behavior is filtered by fundamentally different geomorphic and anthropogenic settings: engineered confinement and restricted sediment connectivity in Surabaya versus open tidal channels and rainfall-sensitive sediment fluxes in Sidoarjo. This finding underscores that correlation-based analyses are highly context-dependent and must be interpreted within typology-specific frameworks rather than regional aggregation alone.

Future research should therefore prioritize: (i) higher-resolution datasets (e.g., Sentinel-2, PlanetScope, UAV imagery) to reduce positional uncertainty and improve EPR reliability; (ii) coupled hydrodynamic–morphodynamic modeling to explicitly represent wave climate, tidal prisms, and river discharge, particularly for open tidal-flat systems; and (iii) typology-specific machine learning models that integrate multiple physical drivers while avoiding distortions introduced by pooled datasets. Strengthening these approaches will improve understanding of how hydroclimatic variability interacts with geomorphology and human modification, supporting more reliable shoreline prediction and adaptive coastal management in tropical regions.

Acknowledgments

The author gratefully acknowledges the BMKG for providing financial and institutional support that made this study possible. This work was developed as part of the ongoing research collaboration between BMKG and ITS, focusing on the integration of geospatial technologies, coastal monitoring, and climate–ocean interaction studies to enhance coastal resilience and adaptive management.

References

- [1] R. J. Nicholls and A. Cazenave, “Sea-level rise and its impact on coastal zones,” *Science*, vol. 328, no. 5985, pp. 1517–1520, 2010. <https://doi.org/10.1126/science.1185782>
- [2] A. Luijendijk, G. Hagenaars, R. Ranasinghe, F. Baart, G. Donchyts, and S. Aarninkhof, “The state of the world’s beaches,” *Scientific Reports*, vol. 8, no. 1, Art. no. 6641, 2018. <https://doi.org/10.1038/s41598-018-24630-6>
- [3] M. I. Vousdoukas *et al.*, “Sandy coastlines under threat of erosion,” *Nature Climate Change*, vol. 10, no. 3, pp. 260–263, 2020. <https://doi.org/10.1038/s41558-020-0697-0>
- [4] R. Almar *et al.*, “Influence of El Niño on the variability of global shoreline change,” *Nature Communications*, vol. 14, Art. no. 38742, 2023. <https://doi.org/10.1038/s41467-023-38742-9>
- [5] T. Sultana, M. T. Islam, M. S. Rahman, A. B. Siddique, and A. N. M. S. Huda, “Evaluating the long-term geomorphic process in relation to hydrodynamics in the central coastal zone of Bangladesh,” *Heliyon*, vol. 9, no. 6, Art. no. e17368, 2023. <https://doi.org/10.1016/j.heliyon.2023.e17368>
- [6] G. Le Cozannet *et al.*, “Sea level change and coastal climate services: The way forward,” *Journal of Marine Science and Engineering*, vol. 5, no. 4, Art. no. 49, 2017. <https://doi.org/10.3390/jmse5040049>
- [7] E. H. Boak and I. L. Turner, “Shoreline definition and detection: A review,” *Journal of Coastal Research*, vol. 21, no. 4, pp. 688–703, 2005. <https://doi.org/10.2112/03-0071.1>
- [8] J. E. Pardo-Pascual, J. Almonacid-Caballer, L. A. Ruiz, and J. Palomar-Vázquez, “Automatic extraction of shorelines from Landsat TM and ETM+ multi-temporal

- images with subpixel precision,” *Remote Sensing of Environment*, vol. 123, pp. 1–11, 2012. <https://doi.org/10.1016/j.rse.2012.02.024>
- [9] E. R. Thieler, E. A. Himmelstoss, J. L. Zichichi, and A. Ergul, *Digital Shoreline Analysis System (DSAS) Version 4.0—An ArcGIS Extension for Calculating Shoreline Change*, U.S. Geological Survey, Open-File Report 2008–1278, 2009. <https://doi.org/10.3133/ofr20081278>
- [10] M. Sengupta, M. R. Ford, P. S. Kench, and G. L. W. Perry, “Exploring the drivers of reef island shoreline change using machine learning models,” *Scientific Reports*, vol. 15, Art. no. 16735, 2025. <https://doi.org/10.1038/s41598-025-00136-w>
- [11] BMKG, *Catatan Iklim dan Kualitas Udara Indonesia 2024*, Badan Meteorologi, Klimatologi, dan Geofisika, 2024. [Online]. Available: <https://iklim.bmkg.go.id/bmkgadmin/storage/buletin/Catatan%20Iklim%20dan%20Kualitas%20Udara%202024%20BMKG.pdf>
- [12] A. Bershadskii, “Hamiltonian distributed chaos in the Asian–Australian monsoons and in the ENSO,” *arXiv preprint arXiv:1805.00397*, 2018. [Online]. Available: <https://arxiv.org/abs/1805.00397>
- [13] S. K. McFeeters, “The use of the Normalized Difference Water Index (NDWI) in the delineation of open water features,” *International Journal of Remote Sensing*, vol. 17, no. 7, pp. 1425–1432, 1996. <https://doi.org/10.1080/01431169608948714>
- [14] F. Xing, Y. P. Wang, and J. Jia, “Hydrodynamics and sediment transport patterns on intertidal flats along middle Jiangsu coast,” *Anthropocene Coasts*, vol. 5, Art. no. 12, 2022. <https://doi.org/10.1007/s44218-022-00012-4>